ID: 718

VISCOSITY AND DENSITY OF ALUMINUM OXIDE NANOLUBRICANT

KEDZIERSKI M. A.
National Institute of Standards and Technology
100 Bureau Drive, Stop 861, Gaithersburg, MD 20899-8631 USA
Mark.Kedzierski@nist.gov

ABSTRACT

This paper presents liquid kinematic viscosity and density measurements of a synthetic polyolester-based aluminum oxide (Al_2O_3) nanoparticle dispersion (nanolubricant) at atmospheric pressure over the temperature range 288 K to 318 K. The polyolester was a commercially available chiller lubricant. Two Al_2O_3 particles diameters were investigated: approximately 60 nm and 10 nm. A good dispersion of the spherical nanoparticles in the lubricant was maintained with a surfactant. Viscosity and density measurements were made for the neat lubricant along with twelve nanolubricants with differing nanoparticle and surfactant mass fractions. The viscosity and the density were shown to increase with respect to increasing nanoparticle mass fraction. The viscosity increased or decreased with surfactant mass fraction depending on the temperature. Correlations of the viscosity and the density are presented as a function of temperature, and nanoparticle and surfactant concentration. The viscosity was also correlated with respect to nanoparticle diameter. The measurements are important for the design of nanolubricants for heat transfer and flow applications.

1. INTRODUCTION

Recent studies by Kedzierski (2008) and Bi et al. (2007) have recommended the use of nanolubricants as a means for improving efficiencies of chillers and refrigerators, respectively. Viscosity measurements of potential nanolubricants for these applications will benefit both fundamental research and design considerations. For example, Kedzierski (2001) has shown that lubricant viscosity significantly influences the performance of boiling refrigerant/lubricant mixtures. The efficiency of the boiling process in a chiller is a key determinant in its overall efficiency. In addition, compressors in refrigerators and chillers have specific requirements for lubricant viscosity. Redesign of either the compressor or the nanolubricant requires nanolubricant viscosity and density measurements to ensure proper lubrication.

Both the size of the nanoparticle and the amount of surfactant used in the manufacture of a nanolubricant are important in determining the quality of the dispersion. In turn, the quality of a dispersion determines the potential for refrigerant boiling enhancement (Kedzierski, 2011) and the thermophysical properties of the nanolubricant. For this reason, the focus of the present study is to investigate the influence of nanoparticle size and the dispersant (surfactant) mass fraction on the viscosity and the density of selected aluminium oxide-based nanolubricants.

2. TEST LIQUIDS

A commercial polyolester lubricant (RL68H)[1], commonly used with R134a chillers, with a nominal liquid kinematic viscosity of 72.3 $mm^2 \cdot s^{-1}$ at 313.15 K, was used as the base lubricant to make twelve different nanolubricants of varying surfactant and nanoparticle mass fractions for two different aluminium oxide (Al_2O_3) nanoparticle diameters (D_p): one with nominally 60 nm, and the other with 10 nm. In addition, the

[1]Certain commercial equipment, instruments, or materials are identified in this paper in order to specify the experimental procedure adequately. Such identification is not intended to imply recommendation or endorsement by the National Institute of Standards and Technology, nor is it intended to imply that the materials or equipment identified are necessarily the best available for the purpose.

viscosity and the density of the neat RL68H and a 50/50 by mass mixture of RL68H and the surfactant were measured.

The size of the Al_2O_3 nanoparticles in the nanolubricant was measured with a Dynamic Light Scattering (DLS) technique using a 633 nm wavelength laser and a sieving technique using a syringe filter. An index of refraction of 1.67 for Al_2O_3 was used in the Brownian motion-based calculation that was done internally by the DLS instrument for the particle size. The uncertainty of the packaged DLS instrumentation was confirmed with a NIST-traceable 60 nm ± 2.7 nm nanofluid standard. The measured diameter of the standard with the DLS system was 64 nm ± 5 nm, which coincides with the range of uncertainty of the standard. The DLS measurements showed that the nanoparticles were well dispersed in the nanolubricant with mostly discrete, nominally 10 nm and 60 nm diameter nanoparticles on a number-weighted basis[2] for the two different nanolubricants. Figure 1 shows a Transmission Electron Microscopy (TEM) image of the 10 nm diameter nanoparticles as taken by Sarkas (2009). The image confirms the good dispersion and shows that the particles are spherical with most of them having diameters of approximately 10 nm or less, but with a few with diameters as large as 50 nm.

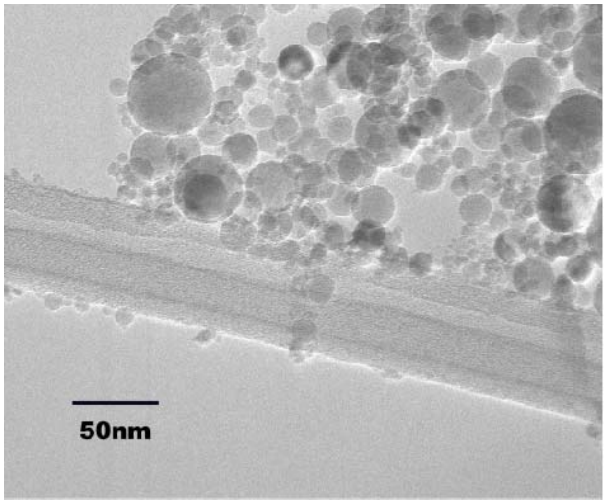

Figure 1. TEM of Al2O3 nanolubricant (Sarkas, 2009).

3. VISCOSITY AND DENSITY MEASUREMENTS

3.1. Rotational Viscometer

A Stabinger-type viscometer (Anton-Parr SVM 3000) was used to measure the dynamic viscosity and the density of the liquid nanolubricant at seven temperatures between approximately 288 K and 318 K. The measurements were made at atmospheric pressure at an approximate altitude of 137 m above sea level (Gaithersburg, Maryland, USA).

The operation principle of the Stabinger-type viscometer relies on rotating concentric cylinders. The liquid sample is contained in the annulus of a concentric cylinder where the inner cylinder is hollow and of less mass than the sample. This allows the inner cylinder to float freely and be centered by centrifugal forces in the sample when the outer cylinder is spun by a rotating magnetic field. Viscous shear forces on the liquid transfer the rotation to the inner cylinder. Measurements on the inner cylinder are used to calculate the difference in speed and torque between the outer and inner cylinder, and thus, the dynamic viscosity. Wasp et al. (1977) have recommended concentric cylinder viscometers for use with solid-liquid suspensions. The viscometer uses a vibrating U-tube to determine the density. The kinematic viscosity reported here is obtained by dividing the dynamic viscosity by the density.

Because the measured viscosity of some fluids may become a function of cylinder angular velocity at high shear rates (Mezger, 2006), the viscosity for the fluid with the highest shear rates obtained from the rotational viscometer was verified with a viscosity measurement with a glass Cannon-Fenske routine viscometer. The average viscosity of the most viscous test fluid (60 nm Al_2O_3 at 0.396 mass fraction) of this study at approximately 297 K measured with the glass viscometer was nearly 7 % larger than that obtained with the rotational viscometer. This 7 % difference in viscosity corresponds to a 0.65 K difference in temperature according to the viscosity correlation for the 60 nm, 0.396 mass fraction nanolubricant. Consequently, a small error in the temperature measurement can have a large effect on the measured viscosity. Despite this, it is believed that the observed difference was primarily due to the nanolubricant film residue that coated the glass-viscometer walls and caused an additional resistance to the flow. Verification

[2]The manufacturer reports these same nanoparticles as having surface-area weighted nanoparticle sizes of 20 nm and 40 nm, which are derived from specific surface area measurements (Sarkas, 2009).

for the least viscous test fluid is supported by the measurements of the neat lubricant in the glass viscometer that agreed with the nominal value reported by the lubricant manufacturer.

3.2. Uncertainties

The viscometer manufacturer-quoted uncertainties for the 95 % confidence level for the kinematic viscosity, the density, and the temperature were ± 0.35 %, ± 0.5 kg·m^{-3}, and ± 0.02 K, respectively. The viscometer was used to measure the density and viscosity of a calibration fluid with a nominal viscosity and density at 293.15 K of 1320 mm^2·s^{-1} and 845.4 kg·m^{-3}, respectively. Residuals between the measurements and the calibration fluid over the same temperature range of this study were within specifications quoted by the manufacturer.

The expanded uncertainties for the kinematic viscosity (U_ν) and density (U_ρ) measurements for each fluid were calculated by combining the manufacturer quoted uncertainty with the standard uncertainties of the regressions for each fluid with a coverage factor. All uncertainties given in this manuscript are for the 95 % confidence level unless otherwise stated. As Table 1 shows, except for three of the data sets, the expanded uncertainty in density (U_ρ) was within ± 0.27 % of the measurement. The largest density uncertainties for a given data set were ± 0.30 %, ± 0.38 %, and ± 1.23 %. Table 2 shows that the uncertainty in the kinematic viscosity, for a given data set, varies between ± 1.7 % and ± 14.6 %. The average U_ν is approximately ± 6.6 %. The uncertainty of the Al_2O_3 mass fractions (x_{np}), the surfactant mass fractions (x_s), and the lubricant mass fractions (x_L) were approximately ± 0.02 %.

Table 1. Linear fit of specific volume with respect to temperature: $\rho_m^{-1}[\mathrm{m^3 \cdot kg^{-1}}] = B_0 + B_1 T[\mathrm{K}]$

x_{np}	x_s	x_L	D_p (nm)	U_ρ (%)	Fitted Constant		Residual standard deviation of fit (%)
					B_0	B_1	
0	0	1.0	N/A	0.24	0.7979×10^{-3}	0.7647×10^{-6}	0.11
0.056	0.014	0.930	10	0.38	0.7689×10^{-3}	0.7164×10^{-6}	0.19
0.056	0.011	0.933	60	0.27	0.7702×10^{-3}	0.7132×10^{-6}	0.13
0.150	0.038	0.812	10	0.25	0.7232×10^{-3}	0.6399×10^{-6}	0.12
0.150	0.030	0.820	60	0.25	0.7224×10^{-3}	0.6429×10^{-6}	0.12
0.250	0.062	0.688	10	0.30	0.6617×10^{-3}	0.5964×10^{-6}	0.15
0.250	0.050	0.700	60	0.23	0.6638×10^{-3}	0.5887×10^{-6}	0.11
0.248	0.078	0.674	10	0.23	0.6707×10^{-3}	0.5945×10^{-6}	0.11
0.244	0.091	0.665	10	0.23	0.6728×10^{-3}	0.5975×10^{-6}	0.11
0.300	0.060	0.640	60	0.21	0.6434×10^{-3}	0.5334×10^{-6}	0.10
0.396	0.079	0.525	60	1.23	0.5870×10^{-3}	0.4767×10^{-6}	0.62
0.392	0.098	0.510	60	0.21	0.5981×10^{-3}	0.4869×10^{-6}	0.10
0.385	0.115	0.500	60	0.21	0.6015×10^{-3}	0.4964×10^{-6}	0.10
0	0.500	0.500	N/A	0.24	0.8211×10^{-3}	0.7607×10^{-6}	0.11
0	1.0	0	N/A	0.34	0.8443×10^{-3}	0.7567×10^{-6}	N/A

4. RESULTS

4.1. Density

Figures 2a and 2b show the measured mixture density (ρ_m) of the nanolubricant mixtures versus temperature (T) at atmospheric pressure for the 10 nm and the 60 nm diameter particles, respectively. The solid lines shown in Figs. 2a and 2b are linear best-fit regressions or estimated means of the data. Thirty-one of the 1812 measurements were removed before fitting because they were identified as "outliers" based on having both high influence and high-leverage (Belsley, et al., 1980). Table 1 gives the constants for the linear regression of the measured specific volume (ρ_m^{-1}) versus the measured temperature for the fluids tested. The dashed lines to either side of the mean represent the lower and upper 95 % simultaneous (multiple-use) confidence intervals for the mean. The last column of Table 1 provides the residual standard deviation of

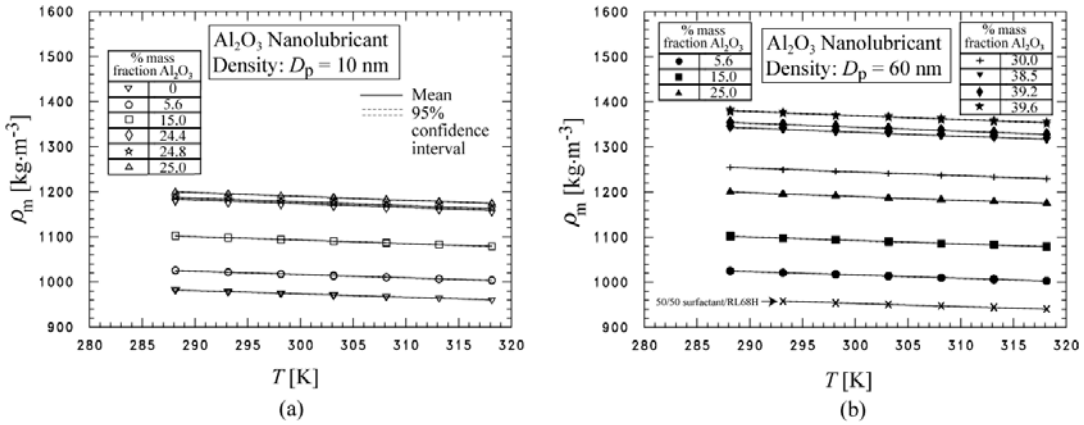

Figure 2. Measured liquid density of Al_2O_3 nanolubricant with 10 nm (a) and 60 nm (b) diameter nanoparticles for various mass fractions at atmospheric pressure.

each fit. The last row of Table 1 gives the fitted constants for the liquid density of the pure surfactant (ρ_s), which were determined by back-substituting the fitted constants for the pure lubricant liquid density (ρ_L), and the fitted constants for the 50/50 mass mixture into eq. (1).

Equation (1) shows the recommended mixture equation for the density of suspensions, ρ_m (Wasp et al., 1977):

$$\frac{1}{\rho_m} = \frac{x_s}{\rho_s} + \frac{x_L}{\rho_L} + \frac{x_{np}}{\rho_{np}} \tag{1}$$

Using the density of the Al_2O_3 nanoparticle ($\rho_{np} = 3600\ kg \cdot m^{-3}$) as reported by Sarkas (2009), the fitted values for ρ_s and ρ_L from Table 1, and the mass fractions corresponding to those of the measured nanolubricant, resulted in deviations from eq. (1) that were within ± 1 % for all of the mixtures and within roughly ± 0.5 % for data with $x_{np} \leq 0.3$. The density residuals were roughly distributed about zero and did not exhibit a temperature dependence, suggesting that the provided value for ρ_{np} was sufficiently accurate and constant for the temperature range of this study. In addition, the density residuals were not a function of nanoparticle diameter, which does not support observations by Grassian (2008) and Jamison et al. (2008) that fundamental properties including density can be size dependent on the nanoscale.

4.2. Viscosity Measurements

Figures 3 and 4 show the measured kinematic viscosity (ν) of the nanolubricant mixtures versus temperature (T) at atmospheric pressure for the 10 nm and the 60 nm diameter particles, respectively. The solid lines shown in the figures are three-parameter best-fit regressions or estimated means of the data to the following form for the normalized viscosity (ν/ν_o),

$$\frac{\nu}{\nu_0} = \exp\left(A_0 + \frac{A_1}{T_r} + A_2 \ln(T_r) + A_3 T_r^{A_4} \right) \tag{2}$$

where ν_o is the unity-viscosity ($\nu_o = 1\ mm^2 \cdot s^{-1}$), and T_r is the nanolubricant temperature normalized by 273.15 K, i.e., $T_r = T/273.15$ K. This form was successfully used for 1944 compounds in the DIPPR Project 801 database (Rowley et al., 2007). The term with the A_3 leading constant was found not to be statistically significant for the present data set and was not used. In addition, 82 of the 1812 measurements were removed before fitting because they were identified as "outliers" based on having both high influence and high-leverage (Belsley, et al., 1980). Table 2 gives the constants for the regression of the normalized kinematic viscosity versus the normalized temperature to eq. (2) for the fluids tested here. The dashed lines in Figs. 3 and 4 to either side of the mean represent the lower and upper 95 % simultaneous (multiple-use) confidence intervals for the mean and is roughly equal to the U_v given in Table 2.

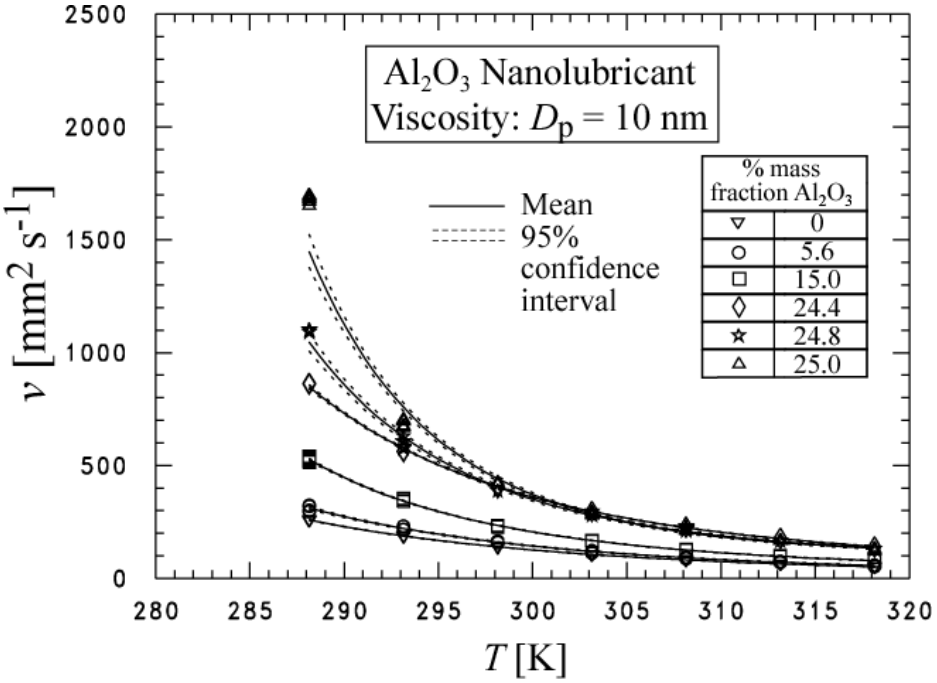

Figure 3. Measured liquid kinematic viscosity of Al_2O_3 nanolubricant with 10 nm diameter nanoparticles for various mass fractions at atmospheric pressure.

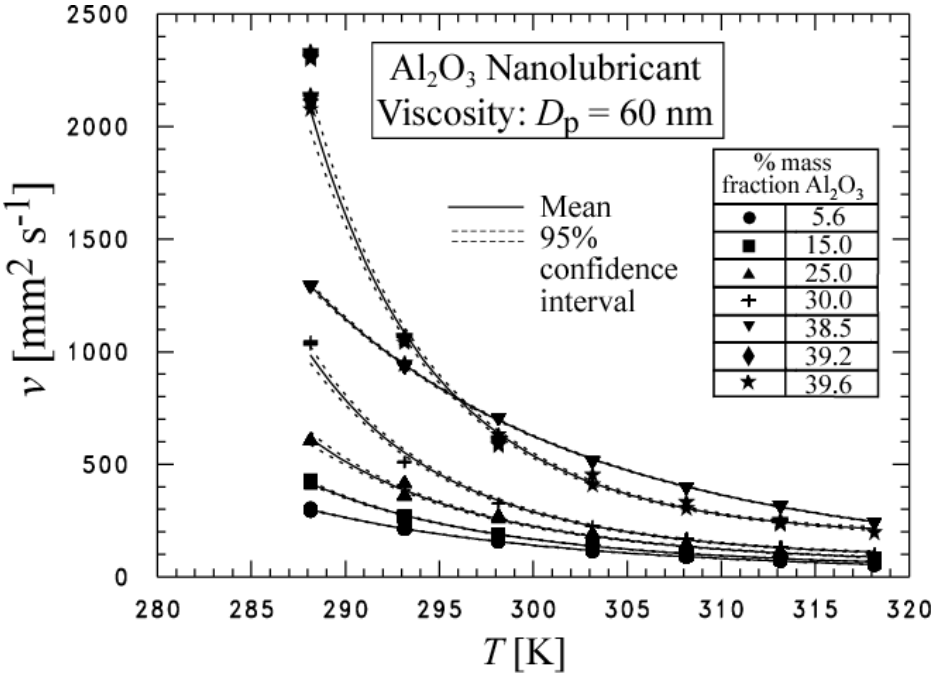

Figure 4. Measured liquid kinematic viscosity of Al_2O_3 nanolubricant with 60 nm diameter nanoparticles for various mass fractions at atmospheric pressure.

Table 2. Viscosity fit with respect to temperature: $\frac{\nu}{\nu_o} = \exp\left(A_0 + \frac{A_1}{T_r} + A_2 \ln T_r \right)$

x_{np}	x_s	x_L	D_p (nm)	U_v (%)	Fitted Constant			Residual standard deviation of fit (%)
					A_0	A_1	A_2	
0	0	1.0	N/A	2.1	-52.1912	58.8418	36.8165	1.0
5.6	0.014	0.930	10	7.5	-69.7768	76.7281	52.0952	3.8
5.6	0.011	0.933	60	2.7	-60.8428	67.7102	44.1411	1.3
15.0	0.038	0.812	10	3.6	-146.202	154.079	119.893	1.8
15.0	0.030	0.820	60	4.2	-147.872	155.481	121.854	2.1
25.0	0.062	0.688	10	14.6	-358.951	368.915	309.006	7.4
25.0	0.050	0.700	60	12.8	-194.279	202.522	163.128	6.5
24.8	0.078	0.674	10	9.6	-237.389	246.384	201.732	4.8
24.4	0.091	0.665	10	2.7	-113.035	121.208	91.3062	1.3
30.0	0.060	0.640	60	9.8	-302.099	311.362	258.869	4.9
39.6	0.079	0.525	60	14.0	-386.581	396.955	335.349	7.1
39.2	0.098	0.510	60	1.7	-68.7064	76.9815	52.4197	0.8
38.5	0.115	0.500	60	2.5	-36.9608	45.1948	23.9985	1.2
0	0.500	0.500	N/A	4.8	-246.727	257.904	208.615	2.4

5. DATA CORRELATION WITH RESPECT TO MASS FRACTION

This section presents the nanolubricant density fit and the correlation of the nanolubricant kinematic viscosity with respect to the temperature, the Al_2O_3 mass fraction (x_{np}), and the surfactant mass fraction.

5.1. Density

Fitting all of the measured densities to a single linear relationship with respect to temperature, nanoparticle mass fraction, and surfactant mass fraction did not produce better agreement with the measurements than eq. (1). As a result, eq. (1) is recommended for predicting the liquid density of the base lubricant, the Al_2O_3 nanolubricants, and the surfactant. Equation (1) is rewritten here using the constants provided in Table 1:

$$\frac{1}{\rho_m}[\mathrm{kg^{-1}\cdot m^3}] = \left(7.647\times10^{-7}(1-x_{np}) - 8.647\times10^{-9}x_s\right)T\,[\mathrm{K}] + 7.979\times10^{-4} - 5.201\times10^{-4}x_{np} + 4.640\times10^{-5}x_s \qquad (3)$$

where the density (ρ_m) has units of $kg\cdot m^{-3}$, and the input temperature (T) has units of K.

5.2. Viscosity

The liquid kinematic viscosity of the base lubricant and the Al_2O_3 nanolubricants (ν_m) were correlated to a modified form of a mixture equation recommended by Reid et al. (1977), which is a mass-fraction-weighted sum of the natural log of the component kinematic viscosities:

$$\ln\nu_m = x_L^{1.25}\ln\nu_L + x_{np}^{1.25}\ln\nu_{np} + x_s^{1.25}\ln\nu_s \qquad (4)$$

The exponents on the mass fractions of eq. (4) were changed from 1, i.e., the exponent recommended by Reid et al. (1977), to 1.25 because it improved the fit of the measurements.

The component kinematic viscosities that are used in eq. (4) are given in the following. The kinematic viscosity of the base lubricant (ν_L) is determined from the equation and coefficients given in Table 1 for $x_L = 1$. The kinematic viscosities of the surfactant (ν_s) and that of the Al_2O_3 nanoparticle (ν_{np}) for eq. (4) are given as:

$$\ln \nu_s = 0.149 D_p[\text{nm}] - 87.2079 + \frac{7.1353}{T_r^{-66.12} + 0.074} \tag{5}$$

$$\ln \nu_{np} = \left(1.426 - 0.0071 D_p[\text{nm}]\right)\left(4.7356 + \frac{1.4706}{T_r^{4.05} - 1.11}\right) \tag{6}$$

where the kinematic viscosity has units of $mm^2 \cdot s^{-1}$, and the diameter of the nanoparticle (D_p) has units of nm.

Equations 5 and 6 do not represent the viscosities of the pure surfactant and the nanoparticles, respectively. Rather, as evident by the D_p term, they are pseudo-viscosities that each account for the interaction between the nanoparticle and the surfactant. This interaction is consistent with the observations of Grassian (2008) and Jamison et al. (2008) who have shown that fundamental properties can be size dependent on the nanoscale.

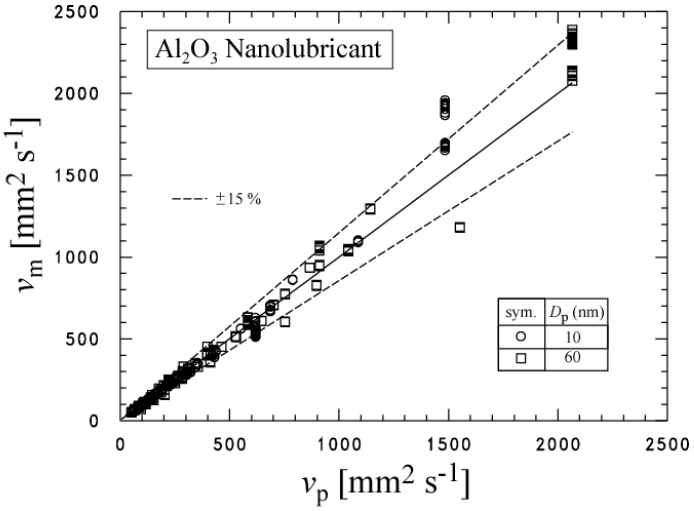

Figure 5. Comparison of measured viscosity of Al_2O_3 nanolubricant to the predictions obtained from eq. (4).

Figure 5 shows the comparison of the measured kinematic viscosity for the liquid nanolubricant to the predictions that were obtained from eq. (4) with eqs. (5) and (6) as input. Ninety-five percent of the viscosities for all of the mixtures (including both nanoparticle sizes) are predicted to within ± 15 % of the measurement, which is consistent with the largest measurement uncertainties given in Table 2.

Surfactants can be used as viscosity modifiers and the effect is typically a function of surfactant concentration (Showell, 2006). Showell (2006) provides one example where a surfactant has no effect on the viscosity for surfactant mass fractions less than 10 %, while causing a nearly 29-fold increase in the viscosity for an increase in the surfactant mass fraction from 20 % to 25 %. Similarly, eq. (4) and Fig. 6 were used to illustrate that the present surfactant has unique effects on the viscosity of the 60 nm nanolubricant. Comparison of the three-dimensional plots in Fig. 6 illustrates that, for temperatures between 300 K and 318 K, an increase in the surfactant mass fraction causes an increase in the nanolubricant viscosity, while the opposite is true for temperatures between approximately 288 K and 300 K. For example, Fig. 6 shows that the viscosity decreases for an increase in the surfactant mass fraction for 288 K. A similar behavior with respect to temperature can be observed for the 10 nm nanolubricant for the same temperature range.

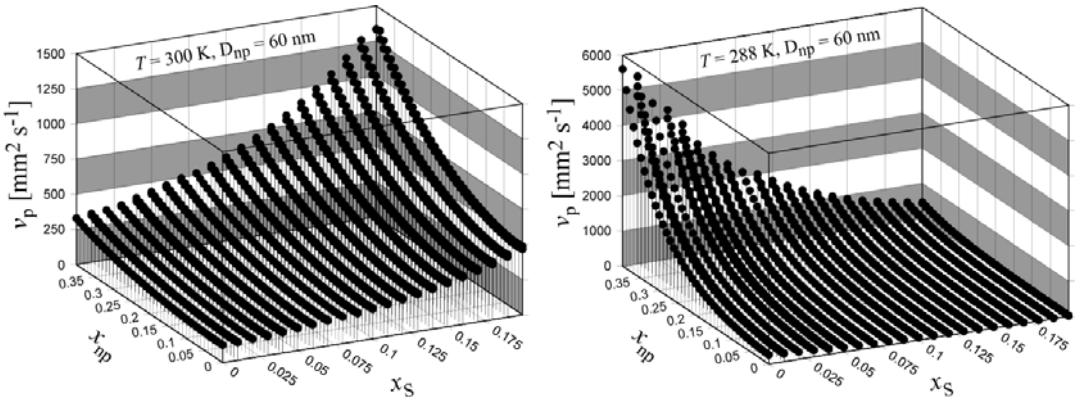

Figure 6. Effect of surfactant mass fraction and temperature on Al_2O_3 nanolubricant viscosity

6. CONCLUSIONS

Liquid kinematic viscosity and liquid density measurements of various synthetic polyolester (chiller lubricant) based aluminum oxide (Al_2O_3) nanoparticle dispersions (nanolubricants) have been presented at atmospheric pressure and for a temperature range from approximately 288 K to 318 K. Two different Al_2O_3 spherical particles diameters were studied (10 nm and 60 nm), which were well dispersed by a surfactant in a commercially available polyolester, chiller lubricant. Viscosity and density measurements were made for the pure base lubricant along with twelve nanolubricants with differing nanoparticle and surfactant mass fractions. The liquid kinematic viscosity was correlated with respect to temperature, nanoparticle mass fraction, surfactant mass fraction, and nanoparticle diameter. Depending on the temperature, the surfactant caused the viscosity of the nanolubricant to either increased or decrease with respect to surfactant mass fraction. A linear relationship was developed for liquid specific volume with respect to temperature. The liquid density decreased with respect to temperature and increased with respect to the Al_2O_3 mass fraction for the temperature range of the study.

7. ACKNOWLEDGEMENTS

This work was funded by NIST. Thanks go to the following NIST personnel for their constructive criticism of the first draft of the manuscript: M. McLinden and A. Persily. The author extends appreciation to Mr. W. Guthrie and Mr. A. Heckert of the NIST Statistical Engineering Division for their consultations on the uncertainty analysis. The viscometer was operated by D. Wilmering of KT Consulting at the NIST laboratory. The nanolubricants were manufactured especially for NIST by Nanophase Technologies using the base lubricant, RL68H, which was supplied by CPI Engineering Services.

8. REFERENCES

Belsley, D. A., Kuh, E., and Welsch, R. E., 1980, Regression Diagnostics: Identifying Influential Data and Sources of Collinearity, Wiley, NY.

Bi, S., Shi, L., and Zhang, L., 2007, Application of Nanoparticles in Domestic Refrigerators, *Applied Thermal Engineering* 28, 1834-1843.

Grassian, V. H., 2008, When Size Really Matters: Size-Dependent Properties and Surface Chemistry of Metal and Metal Oxide Nanoparticles in Gas and Liquid Phase Environments, *J. Phys. Chem. C*, 112 (47), 18303-18313.

Jamison, J. A., Krueger, K. M., Yavuz, C. T., Mayo, J. T., LeCrone, D., Redden, J. J., and Colvin, V. L., 2008, Size-Dependent Sedimentation Properties of Nanocrystals, *ACS Nano*, 2 (2), 311-319.

Kedzierski, M. A., 2011, "Effect of Diamond Nanolubricant on R134a Pool Boiling Heat Transfer," accepted by *Journal of Heat Transfer*

Kedzierski, M. A., 2008, Effect of CuO Nanoparticle Concentration on R134a/Lubricant Pool Boiling Heat Transfer, *ASME Journal of Heat Transfer for the Special Issue of MNHT08*, 131.

Kedzierski, M. A., 2001, The Effect of Lubricant Concentration, Miscibility and Viscosity on R134a Pool Boiling, *Int. J. Refrigeration* 24 (4), 348-366.

Mezger, T. G., 2006, The Rheology Handbook: For Users of Rotational and Oscillatory Rheometers, 2nd Ed., Vincentz, Hannover.

Rowley, R. L., Wilding, W. V., Oscarson, J. L., 2007, DIPPR Project 801 Data Compilation of Pure Compound Properties; March 2007 ed.; AIChE Design Institute for Physical Properties: New York, http://DIPPR.BYU.edu.

Sarkas, H., 2009, Private Communications, Nanophase Technologies Corporation, Romeoville, IL.

Showell, M. S., 2006, Handbook of Detergents Part D: Formulation, Surfactant Science Series V. 128, Taylor and Francis, Boca Raton.

Wasp, E. J., Kenny, J. P., Gandhi, R. L., 1977, Solid-Liquid Flow Slurry Pipeline Transportation, Series on Bulk Materials Handling 1 (4), 56-58.